

Efficient high-energy pulse generation from a diode-side-pumped passively Q-switched Nd:YAG laser and application for optical parametric oscillator

This content has been downloaded from IOPscience. Please scroll down to see the full text.

2014 Laser Phys. Lett. 11 095001

(<http://iopscience.iop.org/1612-202X/11/9/095001>)

View [the table of contents for this issue](#), or go to the [journal homepage](#) for more

Download details:

IP Address: 140.113.38.11

This content was downloaded on 25/12/2014 at 01:32

Please note that [terms and conditions apply](#).

Efficient high-energy pulse generation from a diode-side-pumped passively Q-switched Nd:YAG laser and application for optical parametric oscillator

Y P Huang¹, Y J Huang² and C Y Cho²

¹ Department of Physics, Soochow University, Shih Lin, Taipei 11102, Taiwan

² Department of Electrophysics, National Chiao Tung University, Hsinchu 30010, Taiwan

E-mail: yphuang@scu.edu.tw

Received 17 April 2014, revised 16 June 2014

Accepted for publication 20 June 2014

Published 16 July 2014

Abstract

We employ a convex–concave resonator to develop a high-pulse-energy diode-side-pumped passively Q-switched Nd:YAG laser with high extraction efficiency. At a diode pump energy of 227 mJ, the output laser pulse reaches 30 mJ with a pulse width of 6 ns at a repetition rate of 20 Hz. The optical-to-optical conversion efficiency is up to 13.2%. Based on the developed Nd:YAG laser oscillator, we further employ a monolithic KTP crystal to perform the optical parametric oscillator (OPO). With the 1064 nm input energy of 30 mJ, the OPO energy at 1573 nm is found to be 13.3 mJ, corresponding to an OPO conversion efficiency as high as 44.3%.

Keywords: diode-side-pumped, Q-switched laser, Nd:YAG laser

(Some figures may appear in colour only in the online journal)

1. Introduction

The high gain of Nd:YAG crystal makes it preferred for use in pulsed solid-state lasers [1–4]. Laser resonators with a large mode volume, efficiently utilizing the stored energy in the laser medium, are highly desirable for the generation of high-energy pulses. Two main types of large-mode-volume resonators, unstable resonator [5, 6] and stable telescopic resonator [7], have been implemented to extract the millijoule level pulse with a low divergence angle. Nevertheless, the long-length resonators are not favorable for obtaining short-pulse lasers [8], and typically accompany the problem of alignment sensitivity. Chesler *et al* [9] reported that the convex–concave resonator, in comparison to other resonator types, possesses the advantages of compactness, high efficiency, and insensitivity to perturbations. It is therefore valuable to develop a compact resonator with a large mode volume, based on the convex–concave resonator, for the highly efficient generation of millijoule and nanosecond laser pulses.

Thermal lensing of the laser rod dominantly affects the laser mode volume, stability of laser resonator, and output performances. For diode pumped laser rods, the thermal lensing

is much lower than that of flashlamp pumped [5–7], owing to the thermal loading reduction of laser rods derived from the spectral match [10]. Moreover, quasi-continuous-wave (QCW) laser bars and stacks, giving significantly weaker thermally induced lenses with meter-level focal lengths [11, 12], have been frequently used to achieve multi-millijoule Q-switched neodymium-doped lasers [13–15]. In this work, we employ a convex–concave resonator, in which compact configuration provides a large mode volume, to develop a high-pulse-energy diode-side-pumped passively Q-switched Nd:YAG/Cr⁴⁺:YAG laser with high extraction efficiency. The convex–concave resonator utilizes the property of weak thermal lensing induced by the QCW diode-pumping operation to enter the stable region. At a diode pumped energy of 227 mJ, the output laser pulse reaches 30 mJ with a pulse width of 6 ns at a repetition rate of 20 Hz. The optical-to-optical conversion efficiency is as high as 13.2%. With the developed Nd:YAG laser oscillator, the optical parametric oscillator (OPO) is further investigated with a monolithic KTP crystal in an extracavity configuration. With the 1064 nm input energy of 30 mJ, the OPO energy at 1573 nm is found to be 13.3 mJ. The OPO

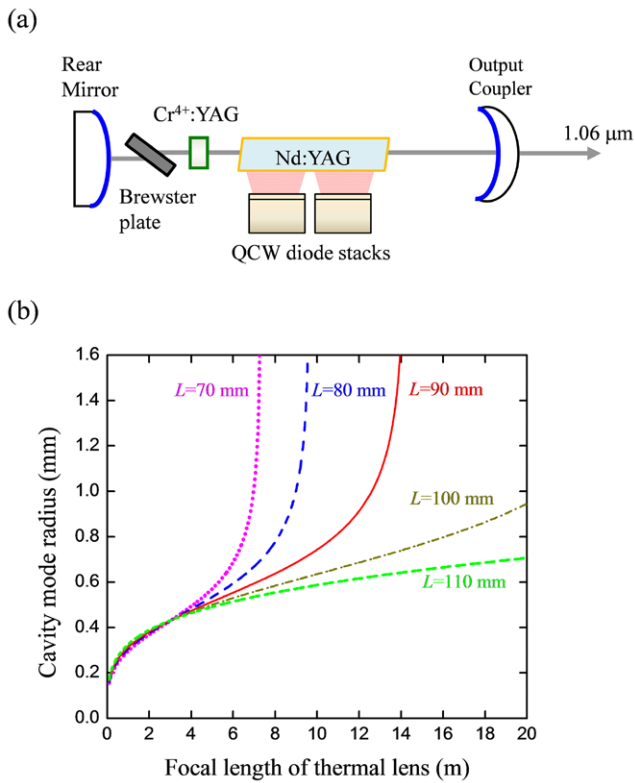


Figure 1. (a) Schematic diagram of the experimental configuration for a QCW diode-side-pumped passively Q-switched Nd:YAG/Cr⁴⁺:YAG laser with a convex–concave resonator. (b) Calculated results for the dependence of the cavity mode sizes on the focal length of the thermal lens for the cases of $L = 70, 80, 90, 100$ and 110 mm.

conversion efficiency is as high as 44.3%, illustrating the excellent performance of the 1064 nm laser oscillator.

2. Passively Q-switched Nd:YAG laser at 1064 nm

2.1. Experimental setup

Figure 1(a) depicts the experimental setup for the QCW diode-side-pumped passively Q-switched Nd:YAG/Cr⁴⁺:YAG laser, employing a convex–concave resonator to make a large mode volume. The pump source was two QCW high-power diode stacks (Coherent G-stack package, Santa Clara, CA, USA). Each diode stack consisted of six 10 mm long diode bars generating a maximum output power of 90 W per bar at the central wavelength of 808 nm. The diode stack was constructed with 400 μm spacing between the diode bars so that the whole emission area was approximately $10 \times 2.4 \text{ mm}^2$. The full divergence angles in the fast and slow axes are approximately 35° and 10°, respectively. The radii of curvature of cavity mirrors are chosen as $R_1 = -500 \text{ mm}$ and $R_2 = 600 \text{ mm}$ for the convex rear mirror and concave output coupler, respectively. The mode radius on a lens-like medium, in the symmetric cavity configuration, was numerically calculated by means of the ABCD matrix method [16]. Figure 1(b) shows the calculated results for the dependences of the cavity mode radius on the focal length of the thermal lens for the cases of cavity length $L = 70, 80, 90, 100$ and 110 mm . It is obvious that, for the

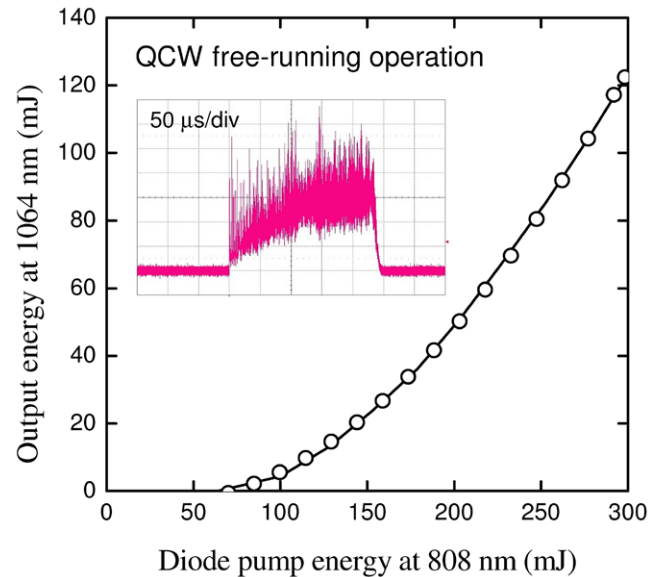


Figure 2. Output energy at 1064 nm with respect to the diode pump energy at 808 nm in the QCW free-running operation. Inset: temporal shape for the laser pulse at the maximum diode pump energy of 298 mJ.

shorter cavity length, the stronger thermal lens is required to step into the stable region and to lase, i.e. the higher pump threshold; whereas the longer cavity length causes the smaller cavity mode radius, which is undesired for the high-energy Q-switched laser. In order to achieve a good cavity design in the QCW diode-pumping operation, we measure the focal length of the induced thermal lens at the incident diode pumped energy of 250 mJ (almost 80% maximum output energy of two diodes driven to emit optical pulse of 300 μs), corresponding to the average pump power of 5 W, using the holographic shear interferometry. The thermal focal length is measured to be in the range of 11–13 m, and thus cavity length $L = 90 \text{ mm}$ is chosen for sufficient energy extraction, which corresponds to the cavity mode radius of 0.82 – 1.08 mm, as depicted in figure 1(b). In addition, the beam waist is numerically calculated to be 0.76 – 1.0 mm on the rear mirror.

The rear mirror was coated for high reflection at 1064 nm ($R > 99.8\%$) on the convex surface. The output coupler, specially designed as a meniscus to collimate the output laser beam, was coated for partial reflection at 1064 nm ($R = 55\%$) on the concave surface and antireflection at 1064 nm ($R < 0.2\%$) on the output convex surface. The gain medium was a 1.0 at. % Nd:YAG crystal with a $4 \times 4 \text{ mm}^2$ cross section and a length of 25 mm, and cut with 2°-wedged end facets to avoid etalon effects. Both end facets of the laser crystal were coated for antireflection at 1064 nm ($R < 0.2\%$), and the pump face was coated for antireflection at 808 nm ($R < 0.2\%$). The pump radiation was directly coupled to the laser crystal without any complex optics. The diode stacks were placed close to the lateral surface of the laser crystal to have good pump efficiency, and they were driven to emit optical pulses of 300 μs to match the upper-level lifetime of Nd:YAG laser crystal. The Cr⁴⁺:YAG crystal with the initial transmission of 30 % was coated for antireflection at 1064 nm on both surfaces ($R < 0.2\%$). The Cr⁴⁺:YAG crystal was placed near the

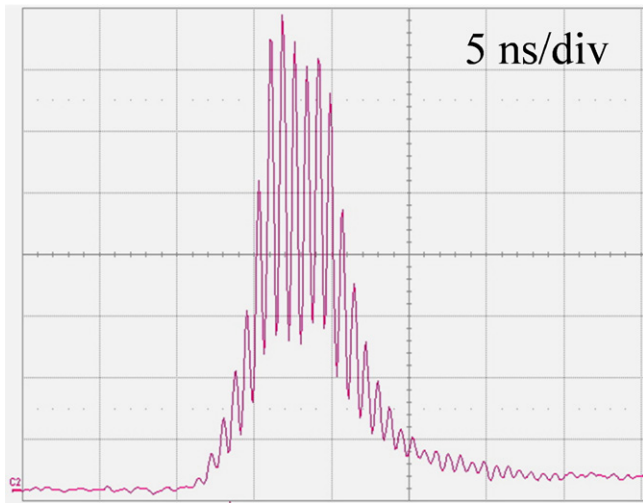


Figure 3. Typical temporal shape for the 1064 nm laser pulse.

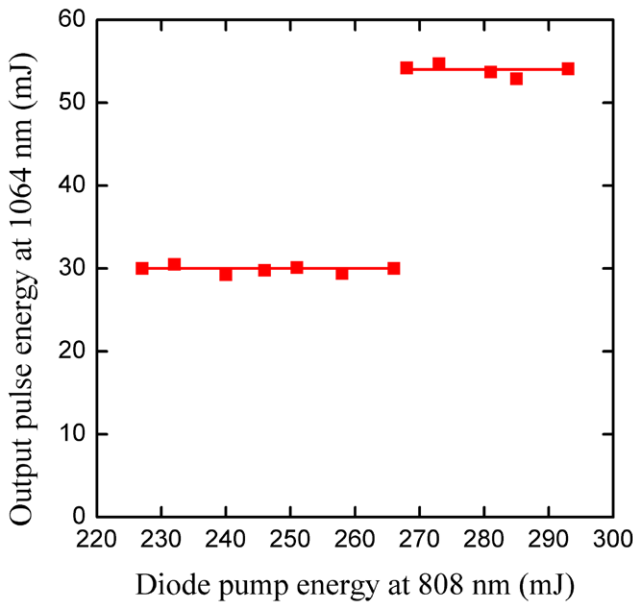


Figure 4. Dependence of the total output energy at 1064 nm on the diode pump energy at 808 nm for the Q-switched operation.

rear mirror where the smaller cavity mode size is. All crystals were wrapped with indium foil and mounted in conductively cooled copper blocks. A Brewster plate was inserted inside the cavity to obtain the linear polarization output. The pulse temporal behavior was recorded by a LeCroy digital oscilloscope (Wavepro 7100, 10 G samples/s, 1 GHz bandwidth) with a fast InGaAs photodiode.

2.2. Experimental results and discussions

First of all, the QCW free-running operation without the Cr⁴⁺:YAG crystal was performed to confirm the reliability of the laser configuration. Figure 2 depicts the experimental results of the output energy as a function of the diode pump energy in the free-running operation. The threshold pump energy is approximately 64 mJ. With a diode pump energy

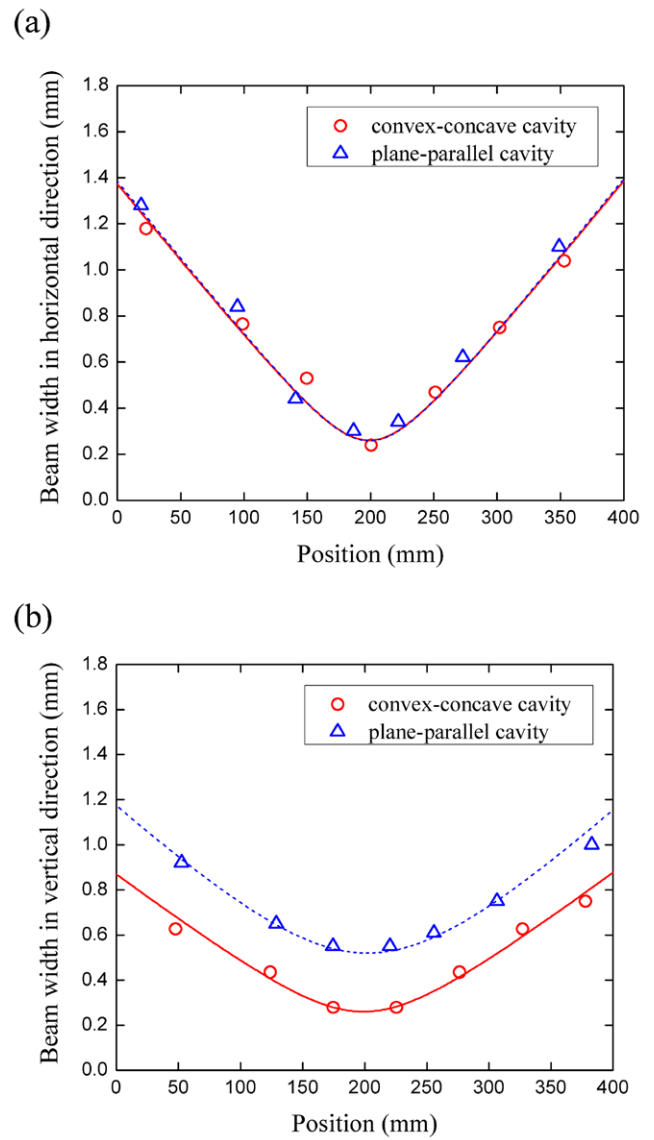


Figure 5. Dependence of the measured beam width at 1064 nm in the (a) horizontal and (b) vertical directions on the position along the propagation direction.

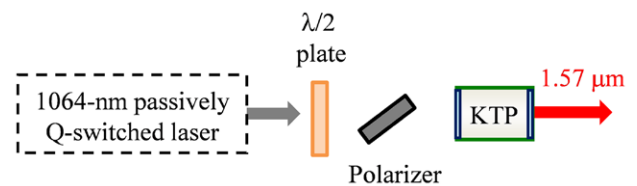


Figure 6. Schematic diagram of the experimental configurations for an extracavity OPO with a monolithic KTP crystal pumped by the developed passively Q-switched Nd:YAG/Cr⁴⁺:YAG laser.

of 298 mJ, the output energy at 1064 nm is 122 mJ, corresponding to an optical-to-optical conversion efficiency of 41%. The temporal shape of the laser pulse, as inserted in figure 2, reveals a train of spikes caused by the relaxation oscillation. The overall slope efficiency is found to be 54%. We then inserted the Cr⁴⁺:YAG crystal into the laser resonator to implement the passively Q-switched Nd:YAG laser.

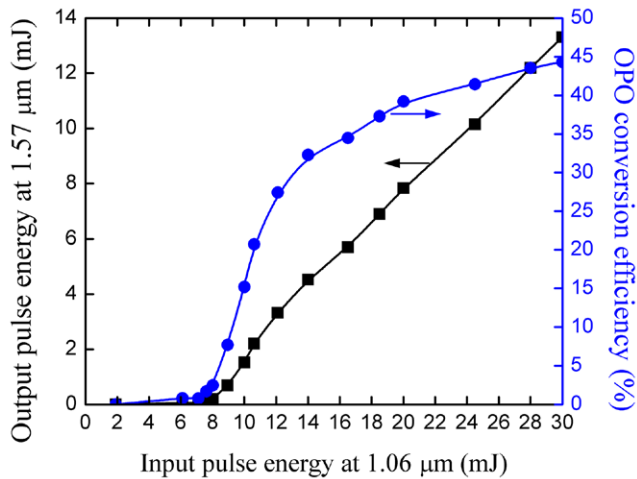


Figure 7. Output pulse energy at $1.57\ \mu\text{m}$ and OPO conversion efficiency as a function of the input pulse energy at $1.06\ \mu\text{m}$.

The threshold pump energy for the Q-switched operation is measured to be approximately 227 mJ, and the output pulse energy at 1064 nm is about 30 mJ at a repetition rate of 20 Hz. It corresponds to an optical-to-optical conversion efficiency of 13.2%. Compared to the results of the passively Q-switched Nd:YAG/Cr⁴⁺:YAG laser with a QCW diode side-pumping system to date [14, 17, 18], the energy extraction efficiency is the highest to our knowledge thanks to the superior cavity design of a convex–concave resonator.

A typical temporal shape of the laser pulse, as depicted in figure 3, displays the mode-locked modulation resulted from the multi-longitudinal mode beating. The separation of the mode-locked pulses is verified to be correspondent with the cavity round-trip frequency of 1.36 GHz. The Q-switched pulse envelope is approximately 6 ns. The Q-switched mode-locked pulses enhance the peak power, which is estimated to be up to 6.3 MW through numerical integration. With increasing the diode pump energy up to 268 mJ, the threshold of absorber bleaching is reached again and double laser pulses appear. Figure 4 shows that the laser output energy step likely increases with the diode pump energy at 808 nm, which connotes that the laser configuration provides the high energy extraction efficiency again. In the single-pulse regime, the laser beam was focused with a 20 cm focal length lens in order to measure the beam quality employing the z-scan method. The beam width was evaluated by the scanning knife-edge method. Figure 5(a, b) show the experimental results of the beam widths in the horizontal and vertical directions as a function of the position along the propagation direction, respectively. Based on the fitting curves in figure 5(a, b), the beam quality factors M^2 are estimated to be 5.0×3.0 (horizontal \times vertical) for the convex–concave cavity [19]. To make a comparison, we also measured the beam quality for a plane-parallel cavity by the above methods, and the results are presented in figure 5(a, b) as well. The M^2 factors are estimated to be 5.2×8.0 (horizontal \times vertical) for the plane-parallel cavity, which represents that the convex–concave cavity provides a significant improvement of beam quality more than twice in the vertical direction. For two kinds of cavities, the

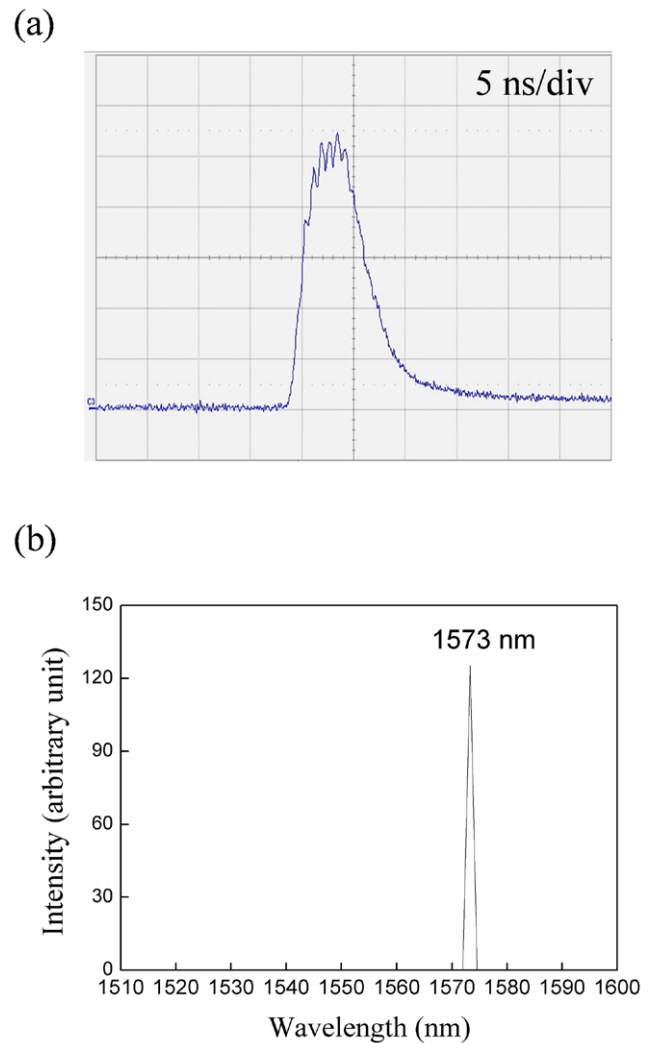


Figure 8. (a) Temporal behavior of the OPO pulse at $1.57\ \mu\text{m}$ with an input pulse energy at $1.06\ \mu\text{m}$ of 30 mJ. (b) Optical spectrum of the OPO.

beam quality in the horizontal direction would be improved by optimization of the diode wavelength and design of the pump coupling. From the comparison, the convex–concave cavity configuration gives the laser oscillator a great beam quality and a low beam divergence, which are beneficial for extracavity wavelength conversions. In the following section, we employ the developed Nd:YAG laser oscillator, operating in the single pulse regime, to explore the performance of the extracavity OPO.

3. Application to extracavity optical parametric oscillator (OPO) at 1573 nm

3.1. Experimental setup

In this experiment, the OPO cavity was formed by a monolithic KTP crystal, as shown in figure 6. The nonlinear crystal KTP with $5 \times 5 \times 25\ \text{mm}^3$ was cut along x axis ($\theta = 90^\circ$ and $\varphi = 0^\circ$) for type-II noncritically phase-matched OPO with the advantages of a maximum effective nonlinear

coefficient and no walk-off effect. For the pump wavelength of $1.06\ \mu\text{m}$, the converted signal and idler wavelengths are near $1.57\ \mu\text{m}$ and $3.1\ \mu\text{m}$, respectively. Owing to the high absorption for wavelengths beyond $3\ \mu\text{m}$ in the KTP crystal, OPO resonator was designed to provide feedback at the signal wavelength of $1.57\ \mu\text{m}$ only, i.e. singly resonant OPO. The pump face of the KTP crystal, acting as the front mirror of the OPO cavity, was coated for high transmission at $1064\ \text{nm}$ ($T > 95\%$) and high reflection at $1573\ \text{nm}$ ($R > 99.8\%$). The other face of the KTP crystal was coated for high reflection at $1064\ \text{nm}$ ($R > 99.8\%$) and partial reflection at $1573\ \text{nm}$ ($R = 80\%$), which enables a double pass of the $1064\ \text{nm}$ input light within the KTP crystal to lower the threshold and to enhance the efficiency for OPO conversion. A slight misalignment of the OPO cavity, replacing the need of an optical isolator, was applied to prevent the feedback of $1064\ \text{nm}$ input light into the laser oscillator. Note that the low-divergence input beam of $1064\ \text{nm}$ leads to the needlessness of collimation optics. An antireflection coated half-waveplate at $1064\ \text{nm}$ and a polarizer were combined to be a variable attenuator for adjusting the input pulse energy at $1064\ \text{nm}$.

3.2. Experimental results and discussions

The dependence of the output pulse energy at $1.57\ \mu\text{m}$ on the input pulse energy at $1.06\ \mu\text{m}$ is shown in figure 7. The OPO threshold energy is approximately $6.0\ \text{mJ}$. With maximum available input energy of $30\ \text{mJ}$ at $1.06\ \mu\text{m}$, the OPO output energy of $13.3\ \text{mJ}$ is obtained, leading to a high slope efficiency of 54.8% . The OPO conversion efficiency is also presented in figure 7 as a function of the input pulse energy at $1.06\ \mu\text{m}$. With increasing the input energy at $1.06\ \mu\text{m}$, the OPO conversion efficiency increases substantially; however, there is a tendency toward saturation at the higher input energy. The maximum OPO conversion efficiency of 44.3% is obtained at the highest input energy of $30\ \text{mJ}$, in which the excellent performance is attributed to the superior cavity design for the $1064\ \text{nm}$ laser oscillator. Figure 8(a) presents the temporal shape of the OPO pulse for the maximum output energy of $13.3\ \text{mJ}$, which exhibits a considerably less pronounced modulation with the same beating frequency as $1064\ \text{nm}$ input pulses. The OPO pulse width is similar to that of the $1064\ \text{nm}$ input pulse of approximately $6\ \text{ns}$. By the numerical integration, the corresponding OPO peak power is calculated to be approximately $2.1\ \text{MW}$. The optical spectrum of OPO, as shown in figure 8(b), was measured with an optical spectrum analyzer (Advantest Q8381A), which has the resolution of $0.1\ \text{nm}$. In addition, the beam-quality M^2 factors of the OPO beam are measured to be less than 3.0 in both directions. The better beam quality than that of the input $1064\ \text{nm}$ beam results from the spatial cleaning effect in the OPO conversion process. It is worth noting that both the eye-safe pulse energy of $13.3\ \text{mJ}$ and the diode-to-signal conversion efficiency of 5.9% , obtained with the extracavity OPO driven by the present side-pumped Nd:YAG laser oscillator, are comparable to those attained with an intracavity OPO scheme by end pumping [20].

4. Conclusions

A compact convex–concave resonator has been demonstrated in a QCW diode-side-pumped passively Q-switched Nd:YAG/Cr⁴⁺:YAG laser. The output pulse energy at $1064\ \text{nm}$ reaches $30\ \text{mJ}$ with a pulse width of $6\ \text{ns}$ at a repetition rate of $20\ \text{Hz}$. The optical-to-optical conversion efficiency is as high as 13.2% . With the developed passively Q-switched Nd:YAG laser, we further investigate the extracavity OPO with a monolithic KTP crystal. The maximum output energy at $1573\ \text{nm}$ of $13.3\ \text{mJ}$ is obtained with a pulse width of $6\ \text{ns}$, corresponding to an OPO conversion efficiency of 44.3% . Efficient extracavity wavelength conversions validates that our compact convex–concave resonator is potentially valuable for the laser oscillator with high extraction efficiency and low beam divergence.

Acknowledgments

The authors thank the National Science Council for their financial support of this research under Grant No. NSC 102-2112-M-031-001-MY3.

References

- [1] Bijanzadeh A R and Khordad R 2009 Study of output energy of Cr⁴⁺:YAG passively Q-switched Nd:YAG laser: using different setups *Opt. Commun.* **282** 2595–603
- [2] Bhandari R and Taira T 2011 $> 6\ \text{MW}$ peak power at $532\ \text{nm}$ from passively Q-switched Nd:YAG/Cr⁴⁺:YAG microchip laser *Opt. Express* **19** 19135–41
- [3] Zhua S Q, Wanga S E, Chena Z Q, Yanga Q G and Pana J 2012 High-power passively Q-switched $532\ \text{nm}$ green laser by using Nd:YAG/Cr⁴⁺:YAG composite crystal *Laser Phys.* **22** 1011–4
- [4] Huang Y P, Huang Y J, Cho C Y and Chen Y F 2013 Influence of output coupling on the performance of a passively Q-switched Nd:YAG laser with intracavity optical parametric oscillator *Opt. Express* **21** 7583–9
- [5] Herbst R L, Komine H and Byer R L 1977 A $200\ \text{mJ}$ unstable resonator Nd:YAG oscillator *Opt. Commun.* **21** 5–7
- [6] Hanna D C and Laycock L C 1979 An unstable resonator Nd:YAG laser *Opt. Quantum Electron.* **11** 153–60
- [7] Hanna D C, Sawyers C G and Yuratich M A 1981 Telescopic resonators for large-volume TEM₀₀-mode operation *Opt. Quantum Electron.* **13** 493–507
- [8] Degnan J J 1989 Theory of the optimally coupled Q-switched laser *IEEE J. Quantum Electron.* **25** 214–20
- [9] Chesler R B and Maydan D 1972 Convex–concave resonators for TEM₀₀ operation of solid-state ion lasers *J. Appl. Phys.* **43** 2254–7
- [10] Hodgson N and Weber H 2005 *Laser Resonators and Beam Propagation* 2nd edn (Berlin: Springer) chapter 13
- [11] Welford D, Rines D M, Dinerman B J and Martinsen R 1992 Observation of enhanced thermal lensing due to near-gaussian pump energy deposition in a laser-diode side-pumped Nd:YAG laser *IEEE J. Quantum Electron.* **28** 1075–80
- [12] Wang S, Eichler H J, Wang X, Kallmeyer F, Ge J, Riesbeck T and Chen J 2009 Diode end pumped Nd:YAG laser at $946\ \text{nm}$ with high pulse energy limited by thermal lensing *Appl. Phys. B* **95** 721–30
- [13] Agnesi A, Pirzio F, Reali G and Piccinno G 2006 Subnanosecond diode-pumped passively Q-switched Nd:GdVO₄ laser with peak power $>1\ \text{MW}$ *Appl. Phys. Lett.* **89** 101120

- [14] Zendzian W, Jabczynski J K and Kwiatkowski J 2008 High peak power Nd:YAG laser pumped by 600-W diode laser stack *Laser Technol.* **40** 441–4
- [15] Huang Y P, Chiang P Y, Huang Y J, Su K W, Chen Y F and Huang K F 2011 High-repetition-rate megawatt millijoule pulses from a Nd:YVO₄ laser passively Q-switched by a semiconductor saturable absorber *Appl. Phys. B* **103** 291–4
- [16] Hodgson N and Weber H 2005 *Laser Resonators and Beam Propagation* 2nd edn (Berlin: Springer) chapter 8
- [17] Afzal R S, Yu A W, Zayhowski T J and Fan T Y 1997 Single-mode high-peak-power passively Q-switched diode-pumped Nd:YAG laser *Opt. Lett.* **22** 1314–6
- [18] Sauder D, Minassian A and Damzen M J 2006 High efficiency laser operation of 2 at. % doped crystal-line Nd:YAG in a bounce geometry *Opt. Express* **14** 1079–85
- [19] Koechner W 2006 *Solid-State Laser Engineering* 6th edn (New York: Springer) chapter 5
- [20] Schilling B W, Chinn S R, Hays A D, Goldberg L and Trussell C W 2006 End-pumped 1.5 μm monoblock laser for broad temperature operation *Appl. Opt.* **45** 6607–15